

Role of van der Waals interactions in adsorption of Xe on Cu(111) and Pt(111)

P. Lazić,¹ Ž. Crljen,¹ R. Brako,¹ and B. Gumhalter²

¹Rudjer Bošković Institute, 10000 Zagreb, Croatia

²Institute of Physics, 10000 Zagreb, Croatia

(Received 15 September 2005; published 5 December 2005)

We consider some recently developed schemes for treating van der Waals interactions within the density functional theory (DFT) on the widely discussed example of adsorption of Xe on Cu(111) and Pt(111) surfaces. Consistent with the overall weakness of the Xe surface and Xe-Xe interactions we assess the performance of the schemes that are appropriate to systems consisting of nearly isolated fragments in which the coefficients of the van der Waals expansion are deduced from DFT calculations. Such generalized DFT calculations of potential energy surfaces yield the structure of Xe adlayers in good agreement with experiments and retrieve the dilation of commensurate monolayer phase in which the intralayer Xe-Xe radial force constants are strongly reduced. This provides a *first principles* interpretation of the observed vibrational properties of adlayers, in general, and the much debated dispersion of in-plane polarized vibrations, in particular.

DOI: 10.1103/PhysRevB.72.245407

PACS number(s): 68.43.Bc, 68.43.Fg, 68.43.Pq, 71.15.Nc

I. INTRODUCTION

A proper theoretical description of the interaction potential in physical adsorption on solid surfaces is a long-standing challenge, of great importance for a large class of problems. For decades the rare gas overlayers have served as benchmark systems of this kind.¹ A popular qualitative picture of the potentials governing physisorption of rare gas atoms has been that of a sum of the long range attractive van der Waals and the short range Pauli repulsion components acting between the electronic charge densities of the substrate and the adatoms.² In many circumstances representation of the total adatom-substrate interaction by the sum of empirical binary potentials has given reasonable results for adsorption energies.³ According to this recipe the highly coordinated lattice sites naturally emerge as preferred adsorption sites for the adatoms. However, recent experiments on the commensurate $(\sqrt{3} \times \sqrt{3})R30^\circ$ Xe monolayers adsorbed on Cu(111)⁴ and Pt(111)⁵ surfaces have contradicted this simple picture in two important aspects: (i) the adsorption sites for Xe atoms deduced from the measurements were on top of the Cu⁶ and Pt^{7,8} atoms instead in the highly coordinated threefold hollow sites, and (ii) the frequencies of in-plane vibrations in monolayer Xe/Cu(111)⁹⁻¹¹ as measured by He atom scattering (HAS) turned out lower than could have been expected from the force constants calculated for *unconstrained* Xe adlayers by using accurate pairwise atomic gas phase potentials.¹² Similar observations were made also for Xe adsorption on Cu(100)¹⁰ and Cu(110)¹³ surfaces. For the Xe/Pt(111) the absence of any significant dispersion of in-plane vibrations in the dilated commensurate Xe monolayer prevented unambiguous assignments of the measured dispersion curves.¹⁴ The attempts to provide a unified interpretation of these findings within the various empirical approaches to physisorption¹⁻³ turned unsuccessful, and resorting to the analysis based on *ab initio* approaches proved indispensable.

The first *ab initio* studies of Ar and Xe adsorption on metals employing the density functional theory-local density

approximation (DFT-LDA) scheme were carried out for a jellium surface.¹⁵ However, for adsorption on real metals a more realistic atomistic representation of the substrate was required. This was undertaken in cluster calculations of adsorption of one and two Xe atoms on a Pt(111) surface within the DFT-LDA,¹⁶ which showed preferred on-top adsorption site, and more recently for on-top Xe adsorption on Cu(111) in the wave function self-consistent field approach, with the inclusion of van der Waals (vdW) attraction as a correlation effect in second order perturbation theory.¹⁷ However, despite the reasonable results obtained for adsorption energy¹⁶ and perpendicular vibration frequency,¹⁷ these calculations proved of a limited use due to the neglect of the periodic structure and band effects.^{18,19}

The role of the substrate periodic electronic structure in the formation of monolayers was investigated in a comparative DFT-LDA and DFT-generalized gradient approximation (GGA) study of $(\sqrt{3} \times \sqrt{3})R30^\circ$ Xe/Pt(111) in Ref. 20. In both cases the binding was strongest at top sites, with LDA overestimating the experimental adsorption energies and vertical adsorbate vibration frequencies, and GGA giving only a shallow and flat adsorption well at large atom-substrate separations. Analogous trends of DFT-LDA and DFT-GGA results were retrieved in a later study of monolayer Xe adsorption on Mg(0001), Al(111), Ti(0001), Cu(111), Pt(111) and Pd(111).²¹ In these works the binding energies calculated using LDA agreed better with the experimental values. However, it is known that the use of LDA functional leads to the overestimate of binding in systems with inhomogeneous electron density, primarily due to an incorrect description of the exchange energy. Hence, the obtained rough agreement of the LDA results with experimental adsorption energies for the studied systems must be considered as accidental, i.e., for these systems the LDA should not be considered as producing more reliable results than the GGA before all important contributions to the total interaction are included.

In the DFT calculations quoted above, the role of intra- and interlayer vdW attraction involving Xe adatoms was not taken into account despite the high Xe dynamic polarizabil-

ity. Hence, for the assessment of validity of the DFT approach the *dynamical polarization* effects that give rise to vdW potentials must be calculated separately but consistently with the obtained electronic densities.

Tractable DFT schemes which include the long-range correlation (and hence the vdW interaction) have been recently developed in Refs. 22–27. Both these approaches are not fully self-consistent, since they use the electron density calculated using a standard DFT functional (usually GGA PW91 or GGA PBE) as a starting point for calculating the energy which includes vdW. This amounts to assuming that the long-range correlation effects, although contributing significantly to the energy of interaction between various parts of the system, are weak enough so that the associated modification of the Kohn–Sham orbitals (and hence of the total electron density) can be neglected.

In the approach of Refs. 22–24 it is assumed that the system consists of well separated “fragments,” e.g. a substrate and a weakly adsorbed atom, and the calculated electron density is used to find the coefficients of (the asymptotic form of) the van der Waals potential between the fragments, which should be added to the energy obtained from DFT calculations. Thus the intrafragment exchange and correlation effects are still included through the standard DFT functional, which is known to work quite well for separate sub-systems (e.g., a metal surface or an atom).

The approach of Refs. 25–27 is more elaborate. The energy is calculated using a DFT functional, in which the exchange–correlation terms are different from the usual ones. In particular, the nonlocal correlation is calculated using an expression which treats on an equal footing the contributions at all distances. The approach aims at providing a “seamless” theory, applicable also to systems which cannot be divided into almost independent fragments. This is clearly an attractive proposal, which may shed light on the role of long-range correlation in strongly interacting systems, once the functional is fully incorporated into the self-consistent calculation of the Kohn–Sham states.

II. INTERFRAGMENT vdW INTERACTIONS

Since the systems which we consider in this paper can be divided into well separated fragments between which only weak interaction remains (Xe–Xe and Xe–substrate), we have first examined how well the approach of Refs. 22–24 works in comparison with the nonasymptotic seamless approach of Refs. 25–27. A well studied system with fragmentation similar as appearing in Xe adlayer is the Kr dimer, for which an accurate empirical interaction potential is available,²⁸ and which has also been investigated by the “seamless” approach (cf. Fig. 2 in Ref. 27). In our calculations we have used the DACAPO program²⁹ with ultrasoft atomic pseudopotentials corresponding to PW91 GGA functional and the plane waves basis. In Fig. 1 we show by dotted lines the interaction energies of Kr₂ (i.e., the difference with respect to two separated atoms) calculated using the PW91, PBE and revPBE GGA functionals. Also shown by a dotted line is the asymptotic vdW term d^{-6} , with the coefficient C_6 taken from Ref. 28. To be more consistent with the spirit of the ap-

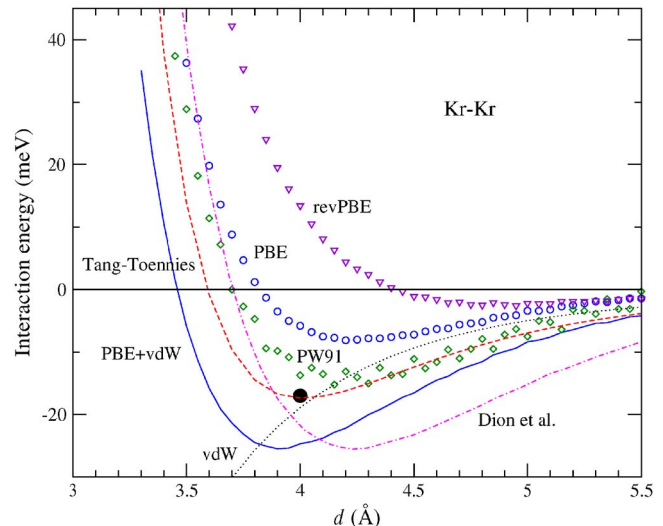


FIG. 1. (Color online) Comparison of different calculations of the interaction potential of a krypton dimer. Symbols: DFT calculations with various flavors of GGA functional. Full line: Our calculation using GGA PBE and “interfragment” vdW contribution. Dash-dot: The seamless calculation of Dion *et al.*²⁷ Dashed line: The parametrized empirical potential of Tang and Toennies.²⁸

proach, we have also calculated C_6 from the DFT electronic densities, using the prescription of Andersson, Langreth, and Lundqvist,²² but the results agreed with the former to within numerical uncertainties. The best agreement with reference results (Tang–Toennies empirical potential and the experimental value of the minimum) is obtained for the sum of the PBE and vdW energies, shown by a full line. The curve is remarkably similar in shape to the seamless result of Dion *et al.*,²⁷ but is shifted towards smaller Kr–Kr distances and therefore agrees better with the experimental data. This indicates that also in the following calculations of interfragment vdW interactions we may expect better results from the PBE rather than the revPBE functional, the exchange part of which is used in the seamless approach of Refs. 25–27.

Next we have calculated interaction energies of an isolated hexagonal Xe layer as a function of the nearest-neighbor distance d , using the DACAPO program. To check the transferability of the electronic density (i.e., the calculation of the electronic density using pseudopotentials and achieving self-consistency with a particular density functional, and then evaluating the energy with another one), we have repeated the calculations employing the ABINIT program³⁰ with norm-conserving native LDA and PBE GGA pseudopotentials.³¹ As shown in Fig. 2 the (non-self-consistent) DACAPO PBE and the (fully self-consistent) ABINIT PBE results agree almost completely. Similar agreement is obtained for the LDA functional (not shown). We have also performed in-layer pairwise summation of the empirical HFD-B2¹² binary Xe–Xe potential, which has been constructed to reproduce the Xe–Xe interactions in gas and condensed phases, and will henceforth consider the resulting sum as equivalent to an experimental quantity. We find that due to large interatomic distances the intralayer vdW interaction is not very sensitive to the model used and hence evaluate it by summing the asymptotic pairwise contribu-

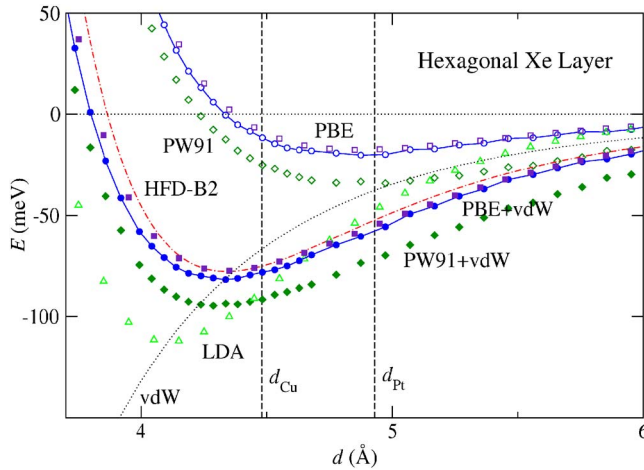


FIG. 2. (Color online) Total DFT-GGA interaction energy (per atom) of an isolated hexagonal layer of Xe atoms calculated as a function of nearest-neighbor distance d without (open symbols) and with addition of the vdW component (full symbols). Circles and squares: PBE functional in ABINIT and DACAPO, respectively, diamonds: PW91 functional, triangles: LDA without vdW. Also shown is the result obtained using empirical HFD-B2 potential. Interatomic distances d_{Cu} and d_{Pt} corresponding to commensurate Xe layers on Cu(111) and Pt(111) surfaces are shown by vertical lines.

tions $-C_6/d_{ij}^{6.22}$ and add it to DFT energies. In this approach the total interaction calculated from the empirical potential is again best reproduced by the combination of PBE and vdW potentials, with the minimum at $d_{\text{min}}=4.3$ Å that nicely correlates with the measured interatomic distances in incommensurate (i.e., unconstrained) Xe monolayers on Cu(111) and Pt(111) at low temperatures.^{4,32} The interatomic distances $d_{\text{Cu}}=4.48$ Å and $d_{\text{Pt}}=4.80$ Å corresponding to commensurate adsorption on Cu(111) and Pt(111), respectively (see below), are also shown. The features of the results in Fig. 2 recur in all our calculations: the interaction energies calculated using GGA exhibit a shallow well with a minimum far out, but with inclusion of the vdW contribution the interaction agrees well with the empirical potential. On the other hand, the calculated LDA potential is largely overbinding even without the inclusion of the vdW attraction and therefore clearly unphysical. Hence, the investigation of its applicability to the adsorption of Xe on Pt and Cu surfaces will not be further pursued in the following.

III. STRUCTURE OF ADSORBED Xe LAYERS

To study Xe adsorption on Cu(111) and Pt(111) surfaces we shall employ DACAPO DFT-GGA scheme complemented with interfragment vdW interactions calculated by using the scheme described in Refs. 22–24. The rationale behind this choice for studying the dynamic polarization interactions in the present systems comes from the best agreement of the results of calculations based on this scheme and the experimental results, as was demonstrated in the preceding section. We first studied monolayer Xe adsorption on Cu(111) surface. The substrate was modeled by six hexago-

nal atomic layers, of which the top three were allowed to relax. The undesired periodicity perpendicular to the surface was remedied by adding a thick vacuum slab above the Xe layer. The fcc lattice constant of the Cu substrate was 3.66 Å, the equilibrium value obtained in our calculations for bulk Cu, which is slightly larger than the experimental value of 3.61 Å. The supercell in x - y coordinates consisted of three Cu atoms in each substrate layer and one Xe atom in the overlayer, which corresponds to the experimentally observed $(\sqrt{3} \times \sqrt{3})R30^\circ$ structure. We have carried out calculations for the various separations z of the Xe layer from the outermost Cu(111) crystal plane. The asymptotic value of the calculated energy for large z is the “desorption energy” of the entire Xe adlayer. To get the energy required to completely dissolve the Xe layer into isolated atoms, we subtracted the cohesive energy of the isolated Xe layer of the same geometry. Note that the experimental desorption energy may be less than that if measured at submonolayer Xe coverages where the average cohesive energy per adatom is smaller.

Next we turn to the nonlocal interaction between the Xe layer and the substrate. According to Refs. 22–24, the van der Waals interaction between an adatom and the slab is

$$E_{\text{vdW}} = -\frac{C_3}{(z - Z_0)^3}, \quad (1)$$

where the coefficient C_3 and the vdW reference plane position Z_0 depend on the dynamic polarization of the substrate and the adatoms. Z_0 is shifted closer to the position of the nuclei of the first Cu layer compared to the static image plane, reflecting the increased importance of the Cu d orbitals in the high-frequency response of the substrate. We assume additive vdW interaction energies between the Xe atoms and the substrate, as we did for the intralayer interactions.

In Fig. 3 we show the results, with and without the vdW contribution, for both PW91 functional and PBE functional (non-self-consistent). The latter gives somewhat better agreement with experimental adsorption energies, but otherwise the two differ only by an almost constant shift in energy. We have carried out the calculations for Xe atoms in on-top, bridge, and hollow positions (fcc hollow and hcp hollow energies are virtually indistinguishable). The calculated DFT energy has a shallow minimum around 4.5 Å, where the bridge configuration has the lowest energy by few meV. However, at distances below 4 Å the on-top site energies are lower due to the adsorption induced rearrangement of the substrate electronic density.^{17,21} Hence, when the interfragment vdW contribution is added (and also the intralayer energy at d_{Cu} from Fig. 2, which gives a constant offset), the on-top site is preferred by few meV, in accord with experiments. The adsorption distance $z_{\text{min}} \approx 3.20$ Å is in good agreement with the experimental value of 3.60 Å,⁶ and the PBE adsorption energy of 250 meV is somewhat larger than the proposed experimental value of 190 meV. Xe adlayer on Cu(111) appears to be at the edge of instability of the incommensurate structure since the energy gain per atom of 3.1 meV, which would be achieved by reducing the Xe-Xe distance to the optimal value d_{min} , is similar to the energy

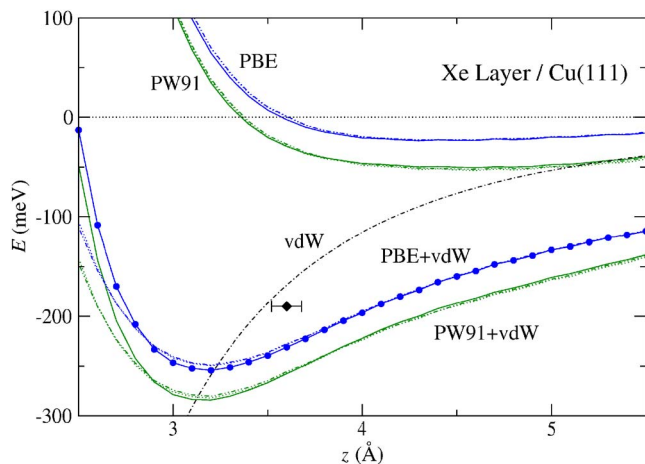


FIG. 3. (Color online) Total interaction energy (per adatom) of commensurate adlayer of Xe on Cu(111) surface calculated using GGA PW91 and PBE functionals (see text), shown as a function of distance z from the last substrate atomic plane. Upper set of curves: DFT results only, lower set: with van der Waals contribution (dash-dot) included. In each set the full, dashed and dotted curves denote results for Xe atoms in on-top, fcc hollow and bridge sites, respectively. The diamond is the experimental value from Refs. 1 and 6.

loss incurred by the fact that some atoms should sit outside on-top sites. The latter quantity is estimated from the energy of various configurations in Fig. 3 at z_{\min} , where the differences between the on-top versus bridge and hollow site configurations are 2.1 and 3.8 meV, respectively. Indeed, experimental indications of a commensurate-incommensurate transition have been detected below 77 K.⁴

Analogous calculations were performed for Xe on Pt(111), using the calculated Pt bulk lattice constant of 4.00 Å, while the experimental one is 3.92 Å. The results shown in Fig. 4 are qualitatively similar to the case of Cu(111). Here the on-top site preference is strongly reinforced by the vdW interaction, and the on-top PBE adsorption energy of 300 meV at $z_{\min}=3.1$ Å is favored by 34.5 meV compared to bridge and 43 meV to hollow site. The on-top commensurate Xe monolayer is nevertheless

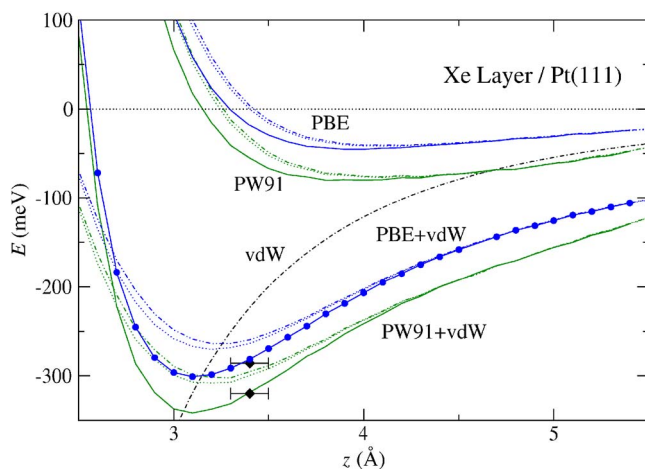


FIG. 4. (Color online) Similar to Fig. 3, but for Xe on Pt(111) surface. Diamonds denote experimental results.^{8,33}

close to instability since the energy per atom due to the intralayer interaction is 23 meV higher at d_{Pt} than at d_{min} (cf. Fig. 2).

IV. VIBRATIONAL PROPERTIES OF Xe ADLAYERS

To discuss the vibrational properties of commensurate Xe adlayers on Cu(111) and Pt(111) we perform the analysis outlined in Refs. 9, 10, and 14, using our calculated potentials. Adsorbed monolayers support three adlayer localized modes or phonons, characterized by the in-surface-plane wave vector \mathbf{Q} and the polarization vector \mathbf{e}_{κ} . The latter is either dominantly perpendicular to \mathbf{Q} and to the surface plane (vertically polarized mode $\kappa=S$), in-plane parallel to \mathbf{Q} (longitudinally polarized mode $\kappa=L$), or in-plane perpendicular to \mathbf{Q} (shear horizontally polarized mode $\kappa=SH$). Experimental S mode frequencies measured by HAS for Xe/Cu(111)^{9,10} and Xe/Pt(111)¹⁴ exhibit practically no dispersion for \mathbf{Q} in the first surface Brillouin zone (SBZ) of the adlayer. Radial force constants β that determine these Einstein-like mode frequencies are calculated from the curvature around the on-top site minima of the potentials shown in Figs. 3 and 4. We find $\beta_{\text{Xe-Cu}}=5.7$ N/m and $\beta_{\text{Xe-Pt}}=12.3$ N/m, yielding $\hbar\omega_S^{\text{Cu}}=3.35$ meV (exp. 2.7 meV⁹) and $\hbar\omega_S^{\text{Pt}}=4.93$ meV (exp. 3.7 meV¹⁴). Here the level of agreement with experiment is the same (Cu) or better (Pt) than in earlier *ab initio* calculations.^{17,20}

The tangential Xe-substrate force constants α which determine L and SH mode frequencies at the SBZ center $\bar{\Gamma}$ ($Q=0$) can be derived from the corrugation of Xe-Cu(111) and Xe-Pt(111) potential energy surfaces, assuming that the most favorable on-top site is the minimum and the bridge and hollow sites are maxima of a two-dimensional cosine potential. We find $\alpha_{\text{Xe-Cu}}=0.134$ N/m and $\alpha_{\text{Xe-Pt}}=1.26$ N/m, giving the $Q=0$ limit of L and SH mode frequencies $\hbar\omega_0^{\text{Cu}}=0.51$ meV and $\hbar\omega_0^{\text{Pt}}=1.58$ meV. The HAS data for L mode are ~ 0.45 meV in Xe/Cu(111),⁹ and 1.7 meV for Xe/Pt(111) (the last value extrapolated from

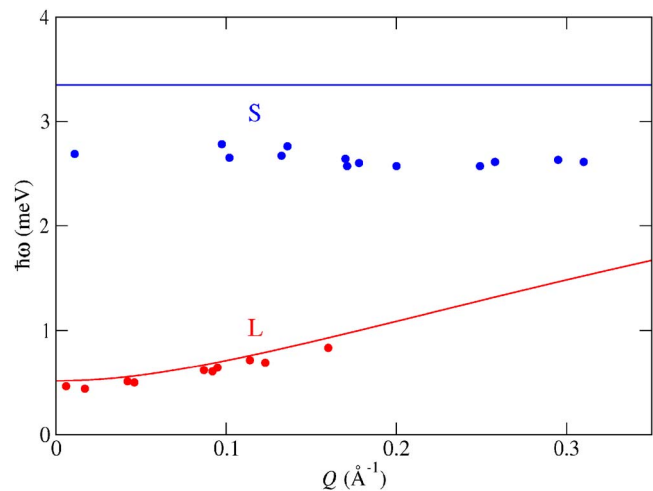


FIG. 5. (Color online) Theoretical Xe-adlayer L and S mode frequencies (lines) compared with experimental values (points) measured in HAS from Xe/Cu(111) in $\bar{\Gamma}\bar{K}$ direction of the adlayer.⁹

$Q \approx 0.2 \text{ \AA}^{-14}$ that is the smallest Q for which the experimental data are available). Dispersion of L mode (and also of SH mode, inaccessible in standard HAS measurements) for $Q > 0$ is dominantly determined by the intralayer radial force constants $\beta_{\text{Xe-Xe}}$.^{9,10,14} Taking that Xe-Xe interaction in *adsorption dilated* Xe adlayers is essentially the same as in isolated Xe layer (Fig. 2); we find $\beta_{\text{Xe-Xe}}(d_{\text{Cu}}) = 0.54 \text{ N/m}$ and $\beta_{\text{Xe-Xe}}(d_{\text{Pt}}) = 0.008 \text{ N/m}$ that in both cases are much lower than at d_{min} for isolated Xe layer. From this we find the dispersion of the L mode in Xe/Cu(111) shown in Fig. 5 that is in excellent accord with HAS data.⁹ For in-plane modes in Xe/Pt(111) we find practically no dispersion, $\hbar\omega^{\text{Pt}}(\mathbf{Q}) \approx \hbar\omega_0^{\text{Pt}}$, also in accord with experiment.¹⁴

V. CONCLUSIONS

In summary, we have demonstrated the necessity of inclusion of van der Waals interactions in the DFT-based calcula-

tions of the potential energy surfaces describing prototype weak adsorption system Xe/metal surfaces. The DFT-GGA approach complemented with a treatment of interfragment vdW forces yields *ab initio* results for the structural and dynamical properties of Xe monolayers on Cu(111) and Pt(111) so far in closest agreement with experiment. This affirms the potentiality of such generalized first principles approach for studying the properties of a wide class of weakly bound fragmented systems, but also calls for extensions of the treatment within a seamless approach²⁵⁻²⁷ which unifies the treatment of dynamic polarization interactions at all interatomic separations.

ACKNOWLEDGMENTS

This work was supported by the Ministry of Science and Technology of the Republic of Croatia under Contract Nos. 0098001 and 0035017.

-
- ¹L. W. Bruch, M. W. Cole, and E. Zaremba, *Physical Adsorption: Forces and Phenomena* (Clarendon Press, Oxford, 1997).
- ²G. Vidali, G. Ihm, H.-Y. Kim, and M. W. Cole, *Surf. Sci. Rep.* **12**, 133 (1991).
- ³W. A. Steele, *Surf. Sci.* **36**, 317 (1973).
- ⁴J. Jupille, J.-J. Erhardt, D. Fargues, and A. Cassuto, *Faraday Discuss. Chem. Soc.* **89**, 323 (1990).
- ⁵K. Kern, R. David, R. L. Palmer, and G. Comsa, *Phys. Rev. Lett.* **56**, 620 (1986).
- ⁶Th. Seyller, M. Caragiu, R. D. Diehl, P. Kaukasoina, and M. Lindroos, *Chem. Phys. Lett.* **291**, 567 (1998).
- ⁷J. M. Gottlieb, *Phys. Rev. B* **42**, R5377 (1990).
- ⁸Th. Seyller, M. Caragiu, R. D. Diehl, P. Kaukasoina, and M. Lindroos, *Phys. Rev. B* **60**, 11084 (1999).
- ⁹J. Braun, D. Fuhrmann, A. Šiber, B. Gumhalter, and Ch. Wöll, *Phys. Rev. Lett.* **80**, 125 (1998).
- ¹⁰A. Šiber, B. Gumhalter, J. Braun, A. P. Graham, M. Bertino, J. P. Toennies, D. Fuhrmann, and Ch. Wöll, *Phys. Rev. B* **59**, 5898 (1999).
- ¹¹B. Gumhalter, *Phys. Rep.* **351**, 1 (2001).
- ¹²A. K. Dham, W. J. Meath, A. R. Allnatt, R. A. Aziz, and M. J. Slaman, *Chem. Phys. Lett.* **142**, 173 (1990).
- ¹³Ch. Boas, M. Kunat, U. Burghaus, B. Gumhalter, and Ch. Wöll, *Phys. Rev. B* **68**, 075403 (2003).
- ¹⁴L. W. Bruch, A. P. Graham, and J. P. Toennies, *Mol. Phys.* **95**, 579 (1999).
- ¹⁵N. D. Lang, *Phys. Rev. Lett.* **46**, 842 (1981).
- ¹⁶J. E. Müller, *Phys. Rev. Lett.* **65**, 3021 (1990).
- ¹⁷P. S. Bagus, V. Staemmler, and Ch. Wöll, *Phys. Rev. Lett.* **89**, 096104 (2002).
- ¹⁸K. Wandelt and B. Gumhalter, *Surf. Sci.* **140**, 355 (1984).
- ¹⁹A. Hotzel, G. Moos, K. Ishioka, M. Wolf, and G. Ertl, *Appl. Phys. B: Lasers Opt.* **68**, 615 (1999).
- ²⁰A. E. Betancourt and D. M. Bird, *J. Phys.: Condens. Matter* **12**, 7077 (2000).
- ²¹J. L. F. Da Silva, C. Stampfl, and M. Scheffler, *Phys. Rev. Lett.* **90**, 066104 (2003); *Phys. Rev. B* **72**, 075424 (2005).
- ²²Y. Andersson, D. C. Langreth, and B. I. Lundqvist, *Phys. Rev. Lett.* **76**, 102 (1996).
- ²³E. Hult, H. Rydberg, B. I. Lundqvist, and D. C. Langreth, *Phys. Rev. B* **59**, 4708 (1999).
- ²⁴E. Hult, P. Hyldgaard, J. Rossmeisl, and B. I. Lundqvist, *Phys. Rev. B* **64**, 195414 (2001).
- ²⁵H. Rydberg, M. Dion, N. Jacobson, E. Schröder, P. Hyldgaard, S. I. Simak, D. C. Langreth, and B. I. Lundqvist, *Phys. Rev. Lett.* **91**, 126402 (2003).
- ²⁶D. C. Langreth, M. Dion, H. Rydberg, E. Schröder, P. Hyldgaard, and B. I. Lundqvist, *Int. J. Quantum Chem.* **101**, 599 (2005).
- ²⁷M. Dion, H. Rydberg, E. Schröder, D. C. Langreth, and B. I. Lundqvist, *Phys. Rev. Lett.* **92**, 246401 (2004).
- ²⁸K. T. Tang and J. P. Toennies, *J. Chem. Phys.* **118**, 4976 (2003).
- ²⁹<http://www.fysik.dtu.dk/campos/Dacapo>
- ³⁰X. Gonze, J.-M. Beuken, R. Caracas, F. Detraux, M. Fuchs, G.-M. Rignanese, L. Sindic, M. Verstraete, G. Zerah, F. Jollet, M. Torrent, A. Roy, M. Mikami, Ph. Ghosez, J.-Y. Raty, and D. C. Allan, *Comput. Mater. Sci.* **25**, 478 (2002).
- ³¹M. Fuchs and M. Scheffler, *Comput. Phys. Commun.* **119**, 67 (1999).
- ³²L. W. Bruch, A. P. Graham, and J. P. Toennies, *J. Chem. Phys.* **112**, 3314 (2000).
- ³³W. Widdra, P. Trischberger, W. Frieß, D. Menzel, S. H Payne, and H. J. Kreuzer, *Phys. Rev. B* **57**, 4111 (1998).